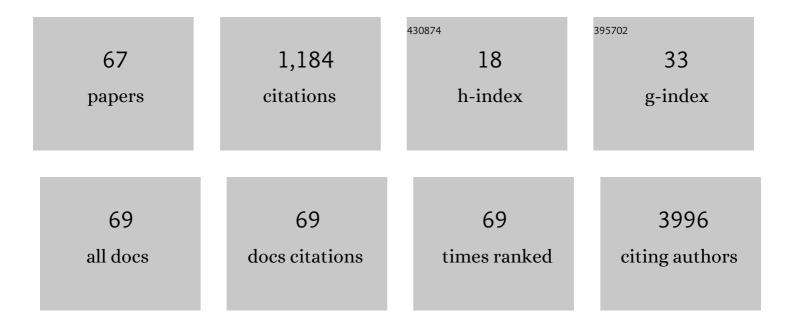
List of Publications by Year in descending order

Source: https://exaly.com/author-pdf/2130278/publications.pdf Version: 2024-02-01



LIN 7 LI

#	Article	IF	CITATIONS
1	Optical Redox Imaging Differentiates Triple-Negative Breast Cancer Subtypes. Advances in Experimental Medicine and Biology, 2021, 1269, 253-258.	1.6	5
2	An Observation on Enhanced Extracellular Acidification and Lactate Production Induced by Inhibition of Lactate Dehydrogenase A. Advances in Experimental Medicine and Biology, 2021, 1269, 163-167.	1.6	3
3	Optical Redox Imaging of Treatment Responses to Nampt Inhibition and Combination Therapy in Triple-Negative Breast Cancer Cells. International Journal of Molecular Sciences, 2021, 22, 5563.	4.1	10
4	Imaging NAD(H) Redox Alterations in Cryopreserved Alveolar Macrophages from Ozone-Exposed Mice and the Impact of Nutrient Starvation during Long Lag Times. Antioxidants, 2021, 10, 767.	5.1	2
5	Potential Biomarker for Triple-Negative Breast Cancer Invasiveness by Optical Redox Imaging. Advances in Experimental Medicine and Biology, 2021, 1269, 247-251.	1.6	3
6	Sex and SP-A2 Dependent NAD(H) Redox Alterations in Mouse Alveolar Macrophages in Response to Ozone Exposure: Potential Implications for COVID-19. Antioxidants, 2020, 9, 915.	5.1	10
7	Two-Photon Autofluorescence Imaging of Fixed Tissues: Feasibility and Potential Values for Biomedical Applications. Advances in Experimental Medicine and Biology, 2020, 1232, 375-381.	1.6	4
8	Rapamycin maintains NAD+/NADH redox homeostasis in muscle cells. Aging, 2020, 12, 17786-17799.	3.1	19
9	Relationship between Optical Redox Status and Reactive Oxygen Species in Cancer Cells. Reactive Oxygen Species (Apex, N C), 2020, 9, 95-108.	5.4	9
10	Commemorating Britton Chance. Molecular Imaging and Biology, 2019, 21, 399-400.	2.6	1
11	Optical Redox Imaging Detects the Effects of DEK Oncogene Knockdown on the Redox State of MDA-MB-231 Breast Cancer Cells. Molecular Imaging and Biology, 2019, 21, 410-416.	2.6	12
12	Optical Redox Imaging of Fixed Unstained Muscle Slides Reveals Useful Biological Information. Molecular Imaging and Biology, 2019, 21, 417-425.	2.6	14
13	Exosomal Thrombospondin-1 Disrupts the Integrity of Endothelial Intercellular Junctions to Facilitate Breast Cancer Cell Metastasis. Cancers, 2019, 11, 1946.	3.7	34
14	Optical Redox Imaging of Lonidamine Treatment Response of Melanoma Cells and Xenografts. Molecular Imaging and Biology, 2019, 21, 426-435.	2.6	16
15	Special Section Guest Editorial: Celebration of the Britton Chance Legacy. Journal of Biomedical Optics, 2019, 24, 1.	2.6	0
16	Differential Expression of PGC1α in Intratumor Redox Subpopulations of Breast Cancer. Advances in Experimental Medicine and Biology, 2018, 1072, 177-181.	1.6	2
17	optical redox imaging of fixed unstained tissue slides to identify biomarkers for breast cancer diagnosis/prognosis: feasibility study. , 2018, 10472, .		1
18	Novel needle redox endoscopy imager for cancer diagnosis. , 2018, 10489, .		1

#	Article	IF	CITATIONS
19	Imaging Redox State in Mouse Muscles of Different Ages. Advances in Experimental Medicine and Biology, 2017, 977, 51-57.	1.6	2
20	A pre-tracer approach for improving the accuracy of metabolic measurements by hyperpolarized nuclear magnetic resonance. Quantitative Imaging in Medicine and Surgery, 2016, 6, 612-614.	2.0	0
21	Optical redox imaging indices discriminate human breast cancer from normal tissues. Journal of Biomedical Optics, 2016, 21, 114003.	2.6	25
22	Potential Indexing of the Invasiveness of Breast Cancer Cells by Mitochondrial Redox Ratios. Advances in Experimental Medicine and Biology, 2016, 923, 121-127.	1.6	31
23	Magnetization Transfer MRI Contrast May Correlate with Tissue Redox State in Prostate Cancer. Advances in Experimental Medicine and Biology, 2016, 923, 401-406.	1.6	3
24	Redox subpopulations and the risk of cancer progression: a new method for characterizing redox heterogeneity. Proceedings of SPIE, 2016, , .	0.8	0
25	Differentiating inflamed and normal lungs by the apparent reaction rate constants of lactate dehydrogenase probed by hyperpolarized (13)C labeled pyruvate. Quantitative Imaging in Medicine and Surgery, 2016, 6, 57-66.	2.0	7
26	Differentiating cancerous from normal breast tissue by redox imaging. , 2015, , .		1
27	Citation analysis of the scientific publications of Britton Chance in ISI citation indexes. Journal of Innovative Optical Health Sciences, 2014, 07, 1430003.	1.0	4
28	ls Higher Lactate an Indicator ofÂTumor Metastatic Risk? A Pilot MRS Study Using Hyperpolarized 13C-Pyruvate. Academic Radiology, 2014, 21, 223-231.	2.5	35
29	Introduction to the Special Issue. Academic Radiology, 2014, 21, 137-138.	2.5	0
30	Quantitative redox imaging biomarkers for studying tissue metabolic state and its heterogeneity. Journal of Innovative Optical Health Sciences, 2014, 07, 1430002.	1.0	23
31	3D imaging of the mitochondrial redox state of rat hearts under normal and fasting conditions. Journal of Innovative Optical Health Sciences, 2014, 07, 1350045.	1.0	10
32	Breast Cancer Redox Heterogeneity Detectable with Chemical Exchange Saturation Transfer (CEST) MRI. Molecular Imaging and Biology, 2014, 16, 670-679.	2.6	27
33	Monitoring Hemodynamic and Metabolic Alterations during Severe Hemorrhagic Shock in Rat Brains. Academic Radiology, 2014, 21, 175-184.	2.5	14
34	Cerebral Hemodynamic Change and Metabolic Alteration in Severe Hemorrhagic Shock. Advances in Experimental Medicine and Biology, 2014, 812, 217-223.	1.6	5
35	Characterizing the metabolic heterogeneity in human breast cancer xenografts by 3D high resolution fluorescence imaging. SpringerPlus, 2013, 2, 73.	1.2	26
36	Redox Imaging of Human Breast Cancer Core Biopsies. Academic Radiology, 2013, 20, 764-768.	2.5	15

#	Article	IF	CITATIONS
37	Imaging heterogeneity in the mitochondrial redox state of premalignant pancreas in the pancreas-specific PTEN-null transgenic mouse model. Biomarker Research, 2013, 1, 6.	6.8	22
38	Ratiometric analysis in hyperpolarized NMR (I): test of the twoâ \in site exchange model and the quantification of reaction rate constants. NMR in Biomedicine, 2013, 26, 1308-1320.	2.8	18
39	CHOP THERAPY INDUCED MITOCHONDRIAL REDOX STATE ALTERATION IN NON-HODGKIN'S LYMPHOMA XENOGRAFTS. Journal of Innovative Optical Health Sciences, 2013, 06, 1350011.	1.0	8
40	REDOX IMAGING OF THE p53-DEPENDENT MITOCHONDRIAL REDOX STATE IN COLON CANCER <i>EX VIVO</i> . Journal of Innovative Optical Health Sciences, 2013, 06, 1350016.	1.0	15
41	Blood Oxygen Level Dependent Magnetization Transfer (BOLDMT) Effect. Advances in Experimental Medicine and Biology, 2013, 765, 31-37.	1.6	2
42	Characterizing Prostate Tumor Mouse Xenografts with CEST and MT-MRI and Redox Scanning. Advances in Experimental Medicine and Biology, 2013, 765, 39-45.	1.6	12
43	In Vivo Metabolic Evaluation of Breast Tumor Mouse Xenografts for Predicting Aggressiveness Using the Hyperpolarized 13C-NMR Technique. Advances in Experimental Medicine and Biology, 2013, 789, 237-242.	1.6	3
44	Mapping the Redox State of CHOP-Treated Non-Hodgkin's Lymphoma Xenografts in Mice. Advances in Experimental Medicine and Biology, 2013, 789, 243-249.	1.6	6
45	Imaging mitochondrial redox potential and its possible link to tumor metastatic potential. Journal of Bioenergetics and Biomembranes, 2012, 44, 645-653.	2.3	28
46	IMAGING REDOX STATE HETEROGENEITY WITHIN INDIVIDUAL EMBRYONIC STEM CELL COLONIES. Journal of Innovative Optical Health Sciences, 2011, 04, 279-288.	1.0	4
47	WORKING WITH AND LEARNING FROM BRIT. Journal of Innovative Optical Health Sciences, 2011, 04, 479-482.	1.0	0
48	Spectral imaging-based methods for quantifying autophagy and apoptosis. Cancer Biology and Therapy, 2011, 12, 349-356.	3.4	15
49	INTRODUCTION TO THE SPECIAL SECTION IN MEMORY OF DR. BRITTON CHANCE. Journal of Innovative Optical Health Sciences, 2011, 04, v-vi.	1.0	0
50	INTRODUCTION – Britton Chance: One of the Most Outstanding Scientists in the World. Journal of Innovative Optical Health Sciences, 2011, 04, v-vii.	1.0	0
51	Measurements of Tumor Cell Autophagy Predict Invasiveness, Resistance to Chemotherapy, and Survival in Melanoma. Clinical Cancer Research, 2011, 17, 3478-3489.	7.0	213
52	Characterizing Breast Cancer Mouse Xenografts with T1ï+MRI. Advances in Experimental Medicine and Biology, 2011, 701, 137-142.	1.6	3
53	Heterogeneity of Mitochondrial Redox State in Premalignant Pancreas in a PTEN Null Transgenic Mouse Model. Advances in Experimental Medicine and Biology, 2011, 701, 207-213.	1.6	19
54	31P-MRS Studies of Melanoma Xenografts with Different Metastatic Potential. Advances in Experimental Medicine and Biology, 2011, 701, 69-73.	1.6	0

#	Article	IF	CITATIONS
55	Quantitative mitochondrial redox imaging of breast cancer metastatic potential. Journal of Biomedical Optics, 2010, 15, 036010.	2.6	80
56	Quantitative magnetic resonance and optical imaging biomarkers of melanoma metastatic potential. Proceedings of the National Academy of Sciences of the United States of America, 2009, 106, 6608-6613.	7.1	86
57	Calibration of CCD-based redox imaging for biological tissues. , 2009, , .		2
58	Calibration of redox scanning for tissue samples. , 2009, , .		7
59	MITOCHONDRIAL REDOX IMAGING FOR CANCER DIAGNOSTIC AND THERAPEUTIC STUDIES. Journal of Innovative Optical Health Sciences, 2009, 02, 325-341.	1.0	53
60	FLUORESCENT IMAGES OF MITOCHONDRIAL REDOX STATES IN <i>IN SITU</i> MOUSE HYPOXIC ISCHEMIC INTESTINES. Journal of Innovative Optical Health Sciences, 2009, 02, 365-374.	1.0	14
61	QUANTITATIVE REDOX SCANNING OF TISSUE SAMPLES USING A CALIBRATION PROCEDURE. Journal of Innovative Optical Health Sciences, 2009, 02, 375-385.	1.0	21
62	Histological Basis Of Mr/Optical Imaging Of Human Melanoma Mouse Xenografts Spanning A Range Of Metastatic Potentials. Advances in Experimental Medicine and Biology, 2009, 645, 247-253.	1.6	17
63	Monitoring response to chemotherapy of nonâ€Hodgkin's lymphoma xenografts by <i>T</i> ₂ â€weighted and diffusionâ€weighted MRI. NMR in Biomedicine, 2008, 21, 1021-1029.	2.8	48
64	Reduced susceptibility effects in perfusion fMRI with single-shot spin-echo EPI acquisitions at 1.5 tesla. Magnetic Resonance Imaging, 2004, 22, 1-7.	1.8	59
65	Magnetic susceptibility quantitation with MRI by solving boundary value problems. Medical Physics, 2003, 30, 449-453.	3.0	11
66	Averaging of harmonic physical fields over an annular region enclosing field sources. American Journal of Physics, 2002, 70, 1029-1033.	0.7	6
67	High-Precision Mapping of the Magnetic Field Utilizing the Harmonic Function Mean Value Property. Journal of Magnetic Resonance, 2001, 148, 442-448.	2.1	38